Odor-based real-time detection and identification of pests and diseases attacking crop plants

Carla C. M. Arce[1†], Marine Mamin[1†], Gregory Röder[1†], Arooran Kanagendran[1], Thomas Degen[1], Emmanuel Defossez[2], Sergio Rasmann[2], Terunobu Akiyama[3], Kosuke Minami[4], Genki Yoshikawa[4,5], Felipe Lopez-Hilfiker[6], Luca Cappellin[6,7], & Ted C. J. Turlings[1*]

[1]Laboratory for Fundamental and Applied Research in Chemical Ecology (FARCE), Institute of Biology, University of Neuchâtel, Rue Emile-Argand 11, 2000 Neuchâtel, Switzerland.
[2]Functional Ecology Laboratory, Institute of Biology, University of Neuchâtel, Rue Emile-Argand 11, 2000 Neuchâtel, Switzerland.
[3]NanoWorld AG, Rue des Saars 10, 2000 Neuchâtel, Switzerland
[4]Research Center for Macromolecules and Biomaterials, National Institute for Materials Science (NIMS), 1-1 Namiki, Tsukuba, Ibaraki 305-0044 Japan
[5]Materials Science and Engineering, Graduate School of Pure and Applied Science, University of Tsukuba, 1-1-1 Tennodai, Tsukuba, Ibaraki 305-8571, Japan
[6]Tofwerk AG, Thun, Switzerland.
[7]Department of Chemical Sciences, University of Padua, Padua, Italy.

lead contact: ted.turlings@unine.ch
[*]corresponding author: ted.turlings@unine.ch
[†]These authors contributed equally to this work

Summary

Plants respond to attacks by herbivores and pathogens by releasing specific blends of volatile compounds and the resulting odor can be specific for the attacking species. We tested if these odors can be used to monitor the presence of pests and diseases in agriculture. Two methods were used, one employing piezoresistive membrane surface stress sensors and the other proton-transfer reaction mass spectrometry. Under laboratory conditions, both techniques readily distinguished between maize plants that were either undamaged, infested by caterpillars, or infected by a fungal pathogen. Under outdoor conditions, the spectrometer could be used to recognize plants with simulated caterpillar damage with about 80% accuracy. Further finetuning of these techniques should lead to the development of odor-sensing mobile devices capable of alerting farmers to the presence and exact location of pests and diseases in their fields.

Keywords: volatile organic compounds, odor sensors, herbivores, pathogens, maize, sustainable agriculture, crop protection.

Introduction

Arguably, the greatest challenge facing humanity is ensuring food security for its ever-growing population. At the same time, it is widely recognized that current agricultural practices are unsustainable and that agriculture is the most important contributor to environmental pollution, the loss of natural habitats and biodiversity, and climate change (*1, 2*). Reducing the use of harmful agrochemicals while optimizing yields should be the primary focus of strategies to overcome these exceedingly detrimental ecological impacts (*3*). As much as 40% of potential crop yields are still lost to pests and diseases (*4*) and strategies to substantially reduce these losses in a sustainable manner are badly needed (*5-7*). We here argue that the early and precise detection of attacks by insects or pathogens within crop fields could be a way to drastically reduce pesticide dependence while still minimizing yield losses. By identifying the exact timing and location of such attacks, farmers should be able to promptly intervene with highly targeted control measures.

Inspired by the fact that plants emit specific volatiles in response to biotic attacks (*8-14*), we investigated the potential application of odor-sensing devices for early pest detection. The induced volatile emissions are part of the plants' dynamic defense responses (*15*), which is triggered by the plants' perception of specific elicitors produced by different attackers (*15-22*). The herbivore-induced plant volatiles serve several ecological functions (*9, 13*), but the role that initially captured the attention of ecologist was their attractiveness to the natural enemies of the herbivores (*23, 24*). The induced volatile blends can be highly specific allowing natural enemies to recognize plants that carry the most suitable prey (*8*). Various elicitors have been identified in the oral secretions of insects (*25-29*) and the first plant receptor for one of these elicitors was recently characterized (*30*). Odor specificity is likely ensured by differences among even the most closely related insect species in the mix of elicitors in their oral secretions (*31*) and by how these elicitors differentially trigger the activation and cross-talk among hormonal signals that mediate plant defense responses (*22, 32*). The current study builds on this specificity in inducible volatile emissions by exploring the use of two odor-sensing devices to detect pest attacks.

We first tested a small device that fits in the palm of a hand. It contains piezoresistive Membrane-type Surface stress Sensors (MSS; Fig. S1A) and employs a micro-fabricated array of thin membranes each with a different receptor layer (*33, 34*). It has been shown that this technique can

be used to detect marker volatiles in patients with head or neck cancer (*35*), but also to measure specific target volatiles from silage (*36*), different liquors (*37*) and herbs (*38*), facilitated by machine-learning based quantification (*39*). The second apparatus that we tested is considerably larger, but more robust and involves proton-transfer reaction time-of-flight mass spectrometry (PTR-TOF-MS; Fig. S1B, Movie S1). The latter technique uses direct chemical ionization of headspace volatiles for on-line detection of volatile organic compounds (*40, 41*). With these two distinctly different odor detection devices we demonstrate the feasibility of developing real-time pest-infestation diagnostics based on plant volatiles.

Results

Odor profiles of caterpillar- and pathogen-infested maize plants

With a conventional volatile collection and analysis techniques (*42*), we determined the volatiles emitted from undamaged maize (*Zea mays*) plants (Fig. 1A), plants infected with the fungus *Colletotrichum graminicola*, and plants infested with caterpillars of the lepidopteran pests *Spodoptera frugiperda* or *Spodoptera exigua* (Fig. 1B). This was done with two commercial hybrids of maize, Delprim and Aventicum. In both cases, undamaged plants released only tiny amounts of either linalool or indole, whereas the infected/infested maize plants released typical blends of inducible volatiles. As can be seen from the chromatograms presented in Fig. 1C, and similar to which have previous reports been reported (*42, 43*), caterpillar-damaged plants released several so-called green leaf volatiles (GLVs; e.g. (*E*)-2-hexenal, (*Z*)-3-hexenol, (*Z*)-3-hexenyl acetate), as well as various inducible terpenoids (e.g. (*E*)-4,8-dimethyl-nonatriene (DMNT), *(E)*-caryophyllene, *(E)*-β-farnesene) and a few aromatic volatiles (e.g. indole, methyl anthranilate) (Fig. 1D).

Further processing of the data using nonmetric multidimensional scaling (NMDS) analysis revealed that the differently treated plants released blends of volatiles that were readily distinguishable from each other (Fig. 2A, PERMANOVA for Delprim, $F_{3,26} = 28.865$, $p = 0.001$, and for Aventicum, $F_{3,28} = 17.662$, $p = 0.001$). Undamaged, pathogen-infected and caterpillar-infested plants released blends of volatiles that were completely distinguishable from each other (Fig. 2A). Although the caterpillar-damaged plants released the same mixture of compounds, the volatiles induced by the two species consistently differ in quantities and, importantly, in ratios (Fig. 1C and 2B; Table S1 and S2). These minor differences in volatile emissions allowed us to

also partially discriminate between the two caterpillar species (Fig. 2A and 2C). A Random Forest (RF) analysis confirmed the odor-based distinction between undamaged, pathogen-infected, and caterpillar-damaged plants with 100% categorization accuracy and that even the two caterpillar species were partially distinguishable (Fig 2C). The distinction between caterpillars was not as evident for the variety Aventicum, showing that selecting sensor-compatible crop genotypes can be important for an odor recognition approach. Overall, these results show that the plants' volatile induced emissions could indeed be exploited for odor-based recognition of plant pests. Plants attacked by the same three antagonists were used for the subsequent evaluations of the two sensing platforms.

Piezoresistive membrane-type surface stress sensors

A Membrane-type Surface stress Sensor (MSS) system (*33*) with twelve independent channels was used to determine differential responsiveness to the odors of plants under attack by the above-mentioned pests. Of the twelve channels, ten worked properly throughout the study and consistently provided signals that could be used for data processing (Table S3). Each of these channels measured the deformation responses of a small silicon membrane that was coated with a different layer of functional silica/titania hybrid nanoparticles or polymers (*34, 37, 44*). The odor of maize plants with the three infestation treatments and of undamaged control plants in the controlled bottle setup (Fig. 1A) were sampled with the MSS setup as demonstrated in Movie S1 and described in detail in the Materials and Methods section. The sampling resulted in distinct signal outputs (Fig. 3A), with each colored line representing the signal from a specific membrane coated with a different polymer (Table S3). Similar to the GC-MS data, the MSS data (electrical outputs in mV, 9 values selected in 1 cycle of 10 seconds sampling; see Material and Methods for details) were subjected to NMDS and RF analyses. The data points clustered in such a manner that each treatment formed clearly distinguishable groups (Fig. 3B). Again, this was slightly better for the variety Delprim than for the variety Aventicum (PERMANOVA for Delprim, $F_{3,59} = 90.086$, $p = 0.001$, and for Aventicum, $F_{3,61} = 66.422$, $p = 0.001$). The RF analysis showed near-perfect to perfect discrimination between undamaged, pathogen-infected and caterpillar-damaged plants (Fig. 3C). Remarkably, the MSS technique could also precisely distinguish between plants attacked by the two closely-related caterpillar species (Fig. 3C).

Proton-transfer reaction mass spectrometry

Our analyses with a proton-transfer-reaction time-of-flight mass spectrometer (PTR-TOF-MS) showed that this real-time measuring technology too can be used to readily distinguish among the odors emitted by maize plants under attack by different antagonists. This was not only achievable in a laboratory setting under clean and controlled airflow (Fig. 4), but also outside, using data from measurements taken on three different days with background odors and turbulent movements of the air (Fig. 5).

In the laboratory, volatile emissions from maize plants attacked by the three above-mentioned pests and untreated control plants were sampled in the same glass bottle system as for the conventional volatile collection technique and the MSS sampling (Fig 1A). Signals (ion counts per second) were relatively stable over the sampling duration (Fig 4A). Further analyses were performed on the 0.9 quantile of the signals over 25 seconds; see Material and Methods for details. Clear quantitative differences were observed between treatments for several ion masses, corresponding notably to the protonated parent ions of benzaldehyde ($C_7H_7O^+$), indole ($C_8H_8N^+$), nonanal ($C_9H_{19}O^+$), DMNT ($C_{11}H_{19}^+$), as well as sesquiterpenes ($C_{15}H_{25}^+$) and their probable fragment ions (Fig 4A, Table S4 and S5). Both NMDS and RF analyses showed that the PTR-TOF-MS output can also be used to distinguish between the odors of the differentially attacked and undamaged plants (Fig. 4B and 4C, PERMANOVA for Delprim, $F_{3,29} = 4.969$, $p = 0.001$, and for Aventicum, $F_{3,29} = 5.965$, $p = 0.001$), albeit somewhat less precisely than with the GC-MS and MSS data. The odor profiles of the two caterpillars were hardly distinguishable from each other. However, the precision with which the processed output could class the correct antagonist was quite satisfactory for the Delprim variety (Fig 4C), especially when using the combined values for the two caterpillar species, which correctly assigned caterpillar-induced odors to the right category with more than 85% accuracy.

Importantly, we showed that under outdoor conditions the PTR-TOF-MS can also readily discriminate between the volatile profile of plants with mimicked caterpillar damage (twice mechanically damaged and treated with caterpillar regurgitant) and the profile of undamaged plants (Fig. 5). In contrast to the laboratory measurements, signals (ion counts per second) were less stable and varied over the duration of measurement (25 seconds, Fig 5A). Further analyses

were performed on the 0.9 quantile of the signals over time; see Material and Methods for details. Although NMDS did not show any separation between damaged and undamaged plants (Fig. S2; PERMANOVA: $F_{1,59}$ =2.116, p = 0.115), a basic RF analysis did already indicate a possible difference between the treatments (Table S6). This was confirmed using an advanced machine learning algorithm, Extreme Gradient Boosting (XGBoost), which allowed us to accurately predict the state of damage suffered by a plant. The XGBoost predictive model was trained with the 10 most discriminatory ion masses, ranked by their importance in an initial model built with all masses quantified in our analysis (Fig. 5B and C). This predictive model yielded an 80% accuracy in discriminating between odors emitted by undamaged and damaged plants (Fig. 5C). The parent ion of indole ($C_8H_{18}N^+$), along with the ions $C_6H_{11}^+$ and $C_7H_9^+$, probable fragments of GLVs and monoterpenes, and the parent ion of DMNT ($C_{11}H_{19}^+$), ranked as particularly important predictors (Fig. 5B). When considered individually, indole ($C_8H_{18}N^+$; Fig. 5A; W = 229, p < 0.001), DMNT ($C_{11}H_{19}^+$; Fig. 5A; W = 287, p = 0.01), and the GLVs fragment ($C_6H_{11}^+$; Fig. 5A; W=282, p = 0.008) were significantly detected more in damaged plants than in undamaged plants. Although the monoterpene fragment ($C_7H_9^+$) was an important predictor, its signal was more variable across treatments (Fig. 5 C; W = 419, p = 0.514). It is important to mention that the model's performance improved by increasing the number of measurements considered for each plant; this improvement already leveled off after two runs of 25 seconds each (Fig. 5D).

Discussion

It is increasingly evident that plants possess sophisticated abilities to selectively produce, perceive and utilize blends of volatile compounds to cope with biotic and abiotic threats (*12-14, 45, 46*). We here show that the plant-produced volatile blends can be used to detect different pest on crops, setting the stage for a novel crop protection strategy.

The concept of using plant odors to monitor the health status of crops is not new (*47-49*) and some systems have been successfully tested under controlled conditions (*50-55*), and as plant-wearable sensor patches(*56*). Also, developments in robotic odor tracking, detection and sampling are highly promising but not yet discriminatory and either short-lived (*57, 58*) or not yet real-time (*59*). Our experiments show that the MSS and the PTR-MS techniques can overcome these shortcomings and that plant-produced volatiles can indeed be used to distinguish among attacks by different

pests in real-time, even under uncontrolled outdoor conditions. Both devices showed great accuracy in distinguishing between the odors from the differently attacked maize plants (Fig. 3 and 4). Importantly, the outdoor measurements show that, even without optimization of the instrument and of the collection set up, and with only a limited number of replicates (n = 30) to train the machine learning model, the PTR-MS technique is already well-suited to differentiate between undamaged and (insect-)damaged plants (Fig 5). More extensive replication will allow the training of more accurate predictive models and even shorter measurement times to evaluate plants in the field.

In the case of the MSS sensor, an analytical model for the dynamic responses to multiple sampling/purging cycles has been established (*60*) but it remains unknown how the differently coated membranes interact with the here tested odor blends. It is therefore not yet clear how each volatile compound contributes to the distinct sensor responses. Even without such mechanistic information on the complex dynamic responses to the odor blends, it is evident that the MSS technology can be used for the accurate detection of specific pests under controlled conditions. Optimizing the collection dynamics and data processing may further reduce measurement times. The MSS, characterized by their small size, ease of use, and cost-effectiveness, hold significant potential for field applications in pest detection. However, their performance in uncontrolled outdoor conditions, especially regarding sensitivity to changes in humidity and temperature, is yet to be explored.

The PTR-MS technology may be less sensitive to changes in environmental conditions (*61*) and, as is evident from our results, can already be employed outdoors (Fig. 5). Importantly, PTR-MS provides genuine real-time information. Moreover, the machine learning approach that we used also allowed us to pinpoint several compounds that can serve as marker volatiles to distinguish among plants that are subject to different biotic stresses. Of these, in the studied maize varieties, indole and DMNT are two of the most indicative inducible compounds to make this distinction, while constitutively released linalool could serve as a reliable background reference. We envision that further targeted measurement that focus on these highly dependable volatiles and possibly incorporating a few additional marker compounds can make this technique truly reliable for odor-based pest and pathogen identification in the maize system. However, current PTR-MS devices are bulky and costly. These limitations might be alleviated if the measurements only target the aforementioned marker volatiles, which would reduce the requirements for mass resolving power

and mass range scanning, theoretically permitting downsizing of the instrument. Mass production for on-farm and other routine applications may further result in a significant reduction in costs.

The use of agricultural robots in the context of sustainable crop protection is realistic, as exemplified by devices that visually recognize weeds in crop fields and then control them either mechanically or with small doses of herbicides. Even in cases where weed-killing chemicals are still used, the amounts are reportedly reduced by more than 90% (*62*). Odor-based pest recognition by robots should result in similar reductions in pesticide use. Pesticides could even be completely replaced by less hazardous control measures, such as the application of insect-killing microbials (*63*) or nematodes (*64*). The proposed precision application could make these more pricy biocontrol approaches also cost-effective.

We conclude that inducible plant volatiles carry specific information that can be readily detected by odor sensors. Further finetuning and modifications of the devices here studied should make it possible to adapt them for field application in agriculture. The envisioned use of agricultural robots equipped with such devices will enable farmers to detect pest insects and diseases on crops long before they do serious harm and will make it possible to effectively and more sustainably eliminate the pests by applying treatments only when and where necessary. We demonstrate that odor-based technologies have clear potential to become part of much needed smart-farming practices that can increase yields while minimizing negative environmental impacts.

Limitations of the study

This study has one primary limitation; because we worked with quarantine pests, we could not study real herbivory under outdoor conditions. Yet, the simulated caterpillar attacks that we applied using their oral secretion is known to trigger the release of similar volatile blends (*24*). Despite the small number of replicates, we were readily able to distinguish this odor from that of healthy plants. Future investigations should prioritize measurements with real herbivory, which can be expected to be even better distinguishable. The MSS sensor was not tested outdoors in this study. We will soon do so in Mexico under fully realistic field conditions with real herbivory.

A minor limitation of our work is that, so far, we used a limited number of replications and plant antagonists on just one plant species. However, the presented proof of principle is expected to

work even better with increased replication and should be applicable to many of the most important pests and diseases, and also for other crops.

Materials and Methods

Plants and growth conditions

Maize plants, *Zea mays var.* Delprim and *var.* Aventicum (seeds supplied by Delley Semences et Plantes SA, CH), were grown in plastic pots (diameter 4 cm; height 10 cm) filled with commercial potting soil (Ricoter, Erdaufbereitung AG, CH) under the standard greenhouse conditions (temperate 26 ± 2°C, relative humidity 60 ± 5%, light was supplemented by using LED lamps with luminous flux (lm) of 8800 with a photoperiod of 16 h). The plants that were used for experiments under laboratory conditions were always kept under greenhouse conditions until being used. For the field measurements, greenhouse-grown plants were placed on the lawn surrounding the greenhouse for 2 to 4 days to acclimatize to field environmental conditions before the experiments were carried out. In all cases, plants were 10 to 12 days old and had 3 to 4 fully developed leaves at the time of the experiments, only plants of similar size were used. They were watered every other day.

Insects, pathogens and regurgitant collection

Caterpillars: In-house colonies of the beet armyworm *Spodoptera exigua* and the fall armyworm *Spodoptera frugiperda* (OFEV permit A140502) caterpillars were reared on a wheat germ-based artificial diet (Frontier Scientific Services, Newark, USA) in transparent plastic boxes under laboratory conditions (temperature 30 ± 5°C, relative humidity 60 - 80%, and 16 h photoperiod) (*65*). For laboratory experiments, second instar *S. exigua* and *S. frugiperda* caterpillars were used to induce the plants.

Fungus: The fungal pathogen *Colletotrichum graminicola* (Ces.) G.W. which causes maize anthracnose leaf blight disease, was used to inoculate maize plants in laboratory experiments. The inoculation of the fungus was based on the method described by Balmer et al. (*66*). Fungal colony (M1.001, obtained from Lisa Vaillancourt, University of Kentucky, Department of Plant Pathology, Lexington, KY) was maintained at 25°C on potato dextrose agar (Difco PDA, Becton Dickinson) under continuous light (70 µE m^{-2} sec^{-1}). Three-week-old plates were used to harvest spores for infection. Twenty µL of a *C. graminicola* conidia suspension (6 × 10^5 spores mL^{-1}

sterile water with 0.01% Silwet L-77, Lehle Seeds) were applied and spread over the leaves using a syringe, four days prior to odor collections. After inoculation, infected plants were kept under room conditions for 16h, without direct sunlight and in an open plastic box (50 × 30 × 35 cm) containing vaporized water used as a humid chamber (min 75% relative humidity, 23 ± 2°C), before transferring them back in an isolated place in the greenhouse. Fungus-inoculated plants were further monitored after scent measurements, as signs of a successful anthracnose leaf blight disease may be hardly detectable at this stage. Plants that had not developed any disease symptoms on day 15 (i.e. a week after inoculation) were excluded from further analyses.

Regurgitant: For field experiment the plants were induced by applying regurgitant of *S. exigua* caterpillars. The regurgitant was collected as previously described (*67*). Before collection, third to fourth instar *S. exigua* caterpillars were fed for 24 h on maize leaves of the same variety and age used in the experiments. Briefly, the head region of a caterpillar was gently squeezed with a pair of featherweight entomology forceps to provoke the release of regurgitant, which was then collected into an Eppendorf tube. The regurgitant was stored at –80°C until use.

Laboratory experiments using GC-MS, MSS and PTR-TOF-MS

Volatile emissions of both maize varieties attacked by different herbivores and pathogens were sampled using three different techniques: Gas Chromatography-Mass Spectrometry (GC-MS), Membrane-type Surface stress Sensor (MSS), and Proton-Transfer-Reaction Time-Of-flight Mass Spectrometry (PTR-TOF-MS).

Gas Chromatography – Mass Spectrometry

To collect volatiles from maize plants (*var.* Delprim and Aventicum) infested either with six *S. exigua* (n = 7-8) or four *S. frugiperda* (n = 7-8) second instar caterpillars per plant. The difference in number was to ensure an equal amount of damage. Volatiles were sampled 24 hours after initial infestation. Plants under pathogenic fungus *C. graminicola* infection (n=8-9) for 7 days were used (see section above for more details). Undamaged maize plants (n=8) were used as control plants. The plants were individually placed in a one-port glass bottle as described by (Turlings et al., 2004). A flow of pure moist air entered each bottle at 0.7 L min^{-1} and the air was pulled through a 25 mg of Porapack Q 80/100 mesh Hayesep-Q adsorbent filter (Ohio Valley Specialist Company, Marietta, USA) at 0.4 L min^{-1}. The volatiles were collected for two hours and then, the filters were

eluted with 150 µL of dichloromethane (Honeywell, Riedel-de Haën, DE), and 10 µL of internal standard was added (*n*-octane and *n*-nonyl acetate, 20 ng/µL each). The samples were stored at −80°C until further analyses.

The volatile samples were analyzed using a gas chromatograph (Agilent 7890B) coupled to a mass spectrometer (Agilent 5977B) in TIC mode. About 1.5 µl of each sample was injected in pulsed split less mode onto an Agilent HP-5MS column (30 m length × 0.25 mm diameter and 0.25-um film thickness). After injection, GC oven temperature was programmed at 40°C for 3 min to 100°C at a rate of 8°C min^{-1}, and subsequently at a rate of 5°C min^{-1} to 230°C. Helium was used as a carrier gas at constant flow of 1.1 mL min^{-1}. The identification and quantification of volatile compounds were performed based on comparing the mass spectra of commercial standards and NIST 17 library spectra.

Membrane-type Surface stress Sensor

Maize plants were either infested with three *S. exigua* (n = 15-18), with two *S. frugiperda* caterpillars (n = 18), or the pathogen *C. graminicola* (n=18; see above sections for details). Control plants received no treatment (n = 12). Each plant was individually placed in a one-port glass bottle previously described (*68*) except that the upper outlet of the vessel was not connected to an adsorbent tube but directly to a nanomechanical Membrane-type Surface stress Sensors module (7.5 × 11.5 × 3 cm, developed by MSS Alliance/Forum (*69, 70*) and provided by National Institute for Materials Science (NIMS), Tsukuba, Japan) with Teflon tubes (50 cm length, 1/16 in / 1mm external/internal diameter). The glass bottle containing the maize plant was connected to the sampling inlet of the MSS module, whereas an empty glass bottle was connected to the purging inlet. The system delivers clean humid air into each bottle during the experiment (see details in the gas chromatograph section). The core of the MSS module contains three arrays, each with four thin membranes (300 µm in diameter), all coated with a different layer of an adsorbent polymer or silica/titania hybrid nanoparticles (Supplementary Table S3). Exposed to a mixture of volatiles, through their interaction with the receptor layer, the shape of each membrane changes in a specific manner. This mechanical strain affects the piezoresistors embedded in the four sensing beams that suspend the membrane. The change in the electric resistances of piezoresistors is then measured by applying a bridge voltage to the full Wheatstone bridge (in mV) (*33*). The bridge voltage was

set to –1.0 V. Measurements are continuous and rely on the alternance of sampling and purging phases defined by the operators.

For the measurements presented here, the micropump in the MSS module was set at 30 cm^3/min (Standard Cubic Centimeters per Minute or SCCM) for both the sampling and the purging flows. For each plant, electrical outputs were measured using a sequence of 10 cycles of sampling (10 sec) - purging (10 sec). The data collection rate was set at 100 Hz, providing 100 electrical outputs per second and per channel. Of the 12 available channels in the module, two showed unstable responses to the volatiles (channels 2.2. and 3.4., for details see Table S3), and were therefore excluded from the analyses. For data analyses, only the sampling phase of the 8^{th} cycle from each sample sequence was used. Within cycle 8, the last 9 seconds were considered (timepoints 141 to 150 sec), which represented 900 data points per channel. A 100 Hz filter was applied, leading to 9 outputs per channel and per plant odor measurement.

Proton-transfer-reaction time-of-flight mass spectrometry (PTR-TOF-MS)

Using a high-resolution PTR-TOF-MS (Vocus S; Tofwerk AG, Thun, CH) we performed real time detection of volatiles from maize plants attacked by either six *S. exigua* caterpillars (n=8), four *S. frugiperda* caterpillars (n=8) or *C. graminicola* pathogen (n=5) (for details see above sections). Undamaged maize plants were used as controls (n=12). The plants were individually placed in a one-port glass bottle as described for the GC-MS and MSS analyses. Air was pulled from the port into the device at a rate of 0.1 l min^{-1} and volatiles protonated through reaction with H_3O^+ ions. Sensitivity of the instrument used in this study is 10000 cps / ppb, and mass resolving power is 7000 m/Δm. Further details about the instrument can be found elsewhere (*61, 71*). In short, the ion-molecule reactor (IMR) conditions during operation were: pressure of 1.8 mbar, temperature of 100°C, and IMR front voltage of 500 V and IMR back voltage 38 V, IMR RF 1.3 MHz, IMR RF amplitude 450 V. Data were recorded using a time resolution of 1 s. The measurements were carried out through the mass to charge ratio (*m/z*) range of 20 - 486. Raw data were processed with Tofware 3.2.3 (Tofwerk AG, Switzerland) for mass calibration and peak fitting. Peaks were targeted based on a list of potential parent and fragment ions of volatiles expected to be released by undamaged and induced maize. This list was built based on our GC-MS results and from literature (Supplementary Table S7). We used the quantile 0.9 from the 25 seconds of at least 1 minute-measurements for each ion quantified to maximize and stabilize the signal.

Real time sampling of volatiles outdoor

We performed real-time detection of the volatiles emitted by undamaged and herbivore-induced plants outdoors, using the same PTR-TOF-MS and parameters described above. This experiment was conducted outside, next to the faculty of science building of the University of Neuchâtel, Switzerland (47°00'00.5"N, 6°57'00.5"E), over three days during summer 2020 (25th of June, 25th of August and 18th of September). Environmental conditions were sunny, with roughly 25 ± 3°C, relative humidity of ca. 60 %, and wind speed of 5 - 8 km h^{-1}. The above environmental parameters were obtained from the MeteoSwiss online platform. All measurements were conducted using fully sun-exposed leaves between 10:00 am and 14:00 pm.

Herbivory was simulated by mechanically damaging the second leaf and then applying caterpillar regurgitant on the wounded area (*67*). The second leaf from each plant was damaged using serrated stainless-steel forceps on both sides of the midrib, in the middle part of the leaf (total damaged area 2 - 3 cm^2) and 8 µL of regurgitant was directly spread on the wounds with a pipette. Healthy plants received no treatment. A first treatment was performed the evening before the measurements (between 16-18 hours) and a second about two hours before the measurements. Plants that were used more than two hours after the second induction were treated a third time. Subsequent wounds were inflicted below the previous ones.

Volatiles were sampled 2 mm above the third leaf, away from the damaged second leave, and therefore mainly capturing systemically released compounds (*72*). We alternated between control (n = 31) and induced (n = 30) plants. All measurements were repeated three times for each single plant, over batches of two to four plants for each treatment. Background volatiles were sampled before each batch. Raw data were processed with Tofware 3.2.1 (Tofwerk AG, Switzerland) for mass calibration and peak fitting. Peaks were targeted based on a list of potential parent and fragment ions of VOCs expected to be released by undamaged and herbivore-induced maize. This list was built based on our GC-MS results and from the literature (Supplementary Table S7). We used the quantile 0.9 from the 25 seconds of ca. 30 to 60 seconds-measurements for each ion quantified to maximize and stabilize the signal.

Data analyses

Analyses were performed with R version 4.3.1.

Laboratory experiments

We apply the same analyses for all indoor experiments to highlight the discriminant efficiency of the three methods (GC-MS, MSS, PTR-TOF-MS). We conducted a nonmetric multidimensional scaling (NMDS) analysis and a permutational multivariate analysis of variance (PERMANOVA) using the vegan package to investigate the separation between the control group and the different types of treatment (*73*). NMDS was based on a Gower dissimilarity matrix and restricted to two dimensions. Additionally, we used a Random Forest (RF) approach to evaluate whether detected compounds or features are potential efficient predictors to discriminate the type of herbivory. Random forest analysis was performed with 150 permutations using the rfPermute package (*74, 75*). The performances of each model were summarized in a confusion matrix generated with the *rfPermute* function. Finally, we also tested independently the effect of treatments on targeted compounds (GC-MS and PTR-TOF-MS data only) using One-way ANOVAs and post-hoc pairwise comparisons with multiple test adjustment (FDR).

Outdoor sampling

Analyses were performed on the quantile 0.9 of peak intensities to remove the noise. Additionally, the data were corrected by a background subtraction (quantile 0.9 for each day of measurement). We first performed NMDS, PERMANOVA and RF analyses as described above. We then used a machine learning approach based on Extreme Gradient Boosting as a classifier (XGBoost package; *76*) to explore the predictability of an insect attack at the individual plant level. To build the predictive model, we first performed a variable selection based on the rank importance of an initial XGBoost model trained with the full set of measurements using the *xgb.importance* function. Variables that ranked in the top 10 were selected to build the predictive model. We further conducted univariate Wilcoxon tests on the four best predictors to examine their individual contributions to the profiles of undamaged and damaged plants. The XGBoost model was set to 500 rounds, with a maximum depth of 5, a learning rate of 0.05, and a binary logistic as “objective” to classify damaged and undamaged individuals. To estimate the predictability of damage, we assessed for each plant the probability of being damaged or not from a model trained recursively on a dataset excluding the targeted plant. Accuracy was summarized in a confusion matrix using the *confusionMatrix* and *fourfoldplot* functions from the caret package (*77*). The performance of

438 the prediction was compared between models built on the quantile 0.9 of a single repetition of
439 measurement for each plant, two or all three repetitions.

440

441 **Acknowledgements**

442 We thank our supportive colleagues in the FARCE group at the University of Neuchâtel for help
443 with insect and plant rearing, laboratory maintenance and helpful discussions. This work was
444 supported by the University of Neuchâtel and advanced grant no. 788949 of the European Research
445 Council awarded to T.C.J.T and in part by Horizon Europe project PurPest, grant no. 101060634.

446

Author contributions

T.C.J.T., C.C.M.A., G.R., A.K., M.M. conceived and designed the project. G.R., C.C. M.A., A.K., M.M. performed experiments. T.A., K.M., G.Y., F.L., L.C. designed sensor equipment and/or provided technical advice. E.D., M.M., G.R., C.C.M.A., A.K., S.R., T.D. conducted and advised on data analyses. T.C.J.T. wrote the manuscript, with contributions from all authors.

Declaration of interests

Several authors have an interest in the commercialization of the devices that were used in this study. The authors declare no other competing interests.

Data and materials availability: Data is available as supplementary material, as well as at https://github.com/ceco-lab/sensor.git, with all R codes.

References

1. J. Poore, T. Nemecek, Reducing food's environmental impacts through producers and consumers. *Science* **360**, 987-992 (2018).
2. F. H. M. Tang, M. Lenzen, A. McBratney, F. Maggi, Risk of pesticide pollution at the global scale. *Nature Geoscience* **14**, 206-210 (2021).
3. N. Möhring *et al.*, Successful implementation of global targets to reduce nutrient and pesticide pollution requires suitable indicators. *Nature Ecology & Evolution* **7**, 1556-1559 (2023).
4. S. Savary *et al.*, The global burden of pathogens and pests on major food crops. *Nature Ecology & Evolution* **3**, 430-439 (2019).
5. H. C. J. Godfray *et al.*, Food security: the challenge of feeding 9 billion people. *Science* **327**, 812-818 (2010).
6. J. Pretty *et al.*, Global assessment of agricultural system redesign for sustainable intensification. *Nature Sustainability* **1**, 441-446 (2018).
7. J. A. Harvey *et al.*, International scientists formulate a roadmap for insect conservation and recovery. *Nature Ecology & Evolution* **4**, 174-176 (2020).
8. C. M. De Moraes, W. J. Lewis, P. W. Paré, H. T. Alborn, J. H. Tumlinson, Herbivore-infested plants selectively attract parasitoids. *Nature* **393**, 570-573 (1998).
9. M. Dicke, I. T. Baldwin, The evolutionary context for herbivore-induced plant volatiles: beyond the 'cry for help'. *Trends in Plant Science* **15**, 167-175 (2010).
10. A. Kessler, M. Heil, The multiple faces of indirect defences and their agents of natural selection. *Functional Ecology* **25**, 348-357 (2011).
11. I. Kaplan, Trophic complexity and the adaptive value of damage-induced plant volatiles. *PLOS Biology* **10**, e1001437 (2012).
12. M. Heil, Herbivore-induced plant volatiles: targets, perception and unanswered questions. *New Phytologist* **204**, 297-306 (2014).

13. T. C. J. Turlings, M. Erb, Tritrophic interactions mediated by herbivore-induced plant volatiles: mechanisms, ecological relevance, and application potential. *Annual Review of Entomology* **63**, 433-452 (2018).
14. M. C. Schuman, Where, when, and why do plant volatiles mediate ecological signaling? The answer is blowing in the wind. *Annual Review of Plant Biology* **74**, 609-633 (2023).
15. E. E. Farmer, *Leaf Defence*. (Oxford University Press, 2014), pp. 226.
16. J. D. G. Jones, J. L. Dangl, The plant immune system. *Nature* **444**, 323-329 (2006).
17. T. Boller, G. Felix, A renaissance of elicitors: perception of microbe-associated molecular patterns and danger signals by pattern-recognition receptors. *Annual Review of Plant Biology* **60**, 379-406 (2009).
18. M. Erb, S. Meldau, G. A. Howe, Role of phytohormones in insect-specific plant reactions. *Trends in Plant Science* **17**, 250-259 (2012).
19. G. W. Felton, J. H. Tumlinson, Plant–insect dialogs: complex interactions at the plant–insect interface. *Current Opinion in Plant Biology* **11**, 457-463 (2008).
20. A. Mithöfer, W. Boland, Recognition of herbivory-associated molecular patterns. *Plant Physiology* **146**, 825-831 (2008).
21. M. Erb, P. Reymond, Molecular interactions between plants and insect herbivores. *Annual Review of Plant Biology* **70**, 527-557 (2019).
22. A. Huffaker *et al.*, Plant elicitor peptides are conserved signals regulating direct and indirect antiherbivore defense. *Proceedings of the National Academy of Sciences of the United States of America* **110**, 5707-5712 (2013).
23. M. Dicke, M. W. Sabelis, How plants obtain predatory mites as bodyguards. *Netherlands Journal of Zoology* **38**, 148–165 (1988).
24. T. C. J. Turlings, J. H. Tumlinson, W. J. Lewis, Exploitation of herbivore-induced plant odors by host-seeking parasitic wasps. *Science* **250**, 1251-1253 (1990).
25. H. T. Alborn *et al.*, Disulfooxy fatty acids from the American bird grasshopper *Schistocerca americana*, elicitors of plant volatiles. *Proceedings of the National Academy of Sciences* **104**, 12976-12981 (2007).
26. H. T. Alborn *et al.*, An elicitor of plant volatiles from beet armyworm oral secretion. *Science* **276**, 945-949 (1997).
27. L. Mattiacci, M. Dicke, M. A. Posthumus, beta-Glucosidase: an elicitor of herbivore-induced plant odor that attracts host-searching parasitic wasps. *Proceedings of the National Academy of Sciences* **92**, 2036-2040 (1995).
28. E. A. Schmelz *et al.*, Fragments of ATP synthase mediate plant perception of insect attack. *Proceedings of the National Academy of Sciences* **103**, 8894-8899 (2006).
29. J. Zeng *et al.*, The N-terminal subunit of vitellogenin in planthopper eggs and saliva acts as a reliable elicitor that induces defenses in rice. *New Phytologist* **238**, 1230-1244 (2023).
30. A. D. Steinbrenner *et al.*, A receptor-like protein mediates plant immune responses to herbivore-associated molecular patterns. *Proceedings of the National Academy of Sciences*, 202018415 (2020).
31. N. Mori *et al.*, Identification of volicitin-related compounds from the regurgitant of lepidopteran caterpillars. *Bioscience, Biotechnology, and Biochemistry* **67**, 1168-1171 (2003).
32. A. Huffaker, N. J. Dafoe, E. A. Schmelz, ZmPep1, an ortholog of *Arabidopsis* Elicitor Peptide 1, regulates maize innate immunity and enhances disease resistance. *Plant Physiology* **155**, 1325-1338 (2011).

33. G. Yoshikawa, T. Akiyama, S. Gautsch, P. Vettiger, H. Rohrer, Nanomechanical Membrane-type Surface Stress Sensor. *Nano Letters* **11**, 1044-1048 (2011).
34. K. Minami, G. Imamura, R. Tamura, K. Shiba, G. Yoshikawa, Recent advances in nanomechanical membrane-type surface stress sensors towards artificial olfaction. *Biosensors*. 2022 (10.3390/bios12090762).
35. H. P. Lang *et al.*, Piezoresistive membrane surface stress sensors for characterization of breath samples of head and neck cancer patients. *Sensors (Basel)* **16**, 1149 (2016).
36. K. Minami *et al.*, Measurement of volatile fatty acids in silage through odors with nanomechanical sensors. *Biosensors*. 2023 (10.3390/bios13020152).
37. K. Shiba, R. Tamura, G. Imamura, G. Yoshikawa, Data-driven nanomechanical sensing: specific information extraction from a complex system. *Scientific Reports* **7**, 3661 (2017).
38. G. Imamura, K. Shiba, G. Yoshikawa, T. Washio, Free-hand gas identification based on transfer function ratios without gas flow control. *Scientific Reports* **9**, 9768 (2019).
39. K. Shiba *et al.*, Functional nanoparticles-coated nanomechanical sensor arrays for machine learning-based quantitative odor analysis. *ACS Sensors* **3**, 1592-1600 (2018).
40. A. Jordan *et al.*, A high resolution and high sensitivity proton-transfer-reaction time-of-flight mass spectrometer (PTR-TOF-MS). *International Journal of Mass Spectrometry* **286**, 122-128 (2009).
41. M. Graus, M. Müller, A. Hansel, High resolution PTR-TOF: quantification and formula confirmation of voc in real time. *Journal of the American Society for Mass Spectrometry* **21**, 1037-1044 (2010).
42. M. D'Alessandro, T. C. J. Turlings, Advances and challenges in the identification of volatiles that mediate interactions among plants and arthropods. *The Analyst* **131**, 24-32 (2006).
43. T. C. J. Turlings, U. B. Lengwiler, M. L. Bernasconi, D. Wechsler, Timing of induced volatile emissions in maize seedlings. *Planta* **207**, 146-152 (1998).
44. K. Shiba, T. Sugiyama, T. Takei, G. Yoshikawa, Controlled growth of silica–titania hybrid functional nanoparticles through a multistep microfluidic approach. *Chemical Communications* **51**, 15854-15857 (2015).
45. M. C. Mescher, C. M. De Moraes, Role of plant sensory perception in plant–animal interactions. *Journal of Experimental Botany* **66**, 425-433 (2014).
46. I. T. Baldwin, Plant volatiles. *Current Biology* **20**, R392-R397 (2010).
47. S. Li, A. Simonian, B. A. Chin, Sensors for agriculture and the food industry. *The Electrochemical Society Interface* **19**, 41-46 (2010).
48. A.-K. Mahlein, E.-C. Oerke, U. Steiner, H.-W. Dehne, Recent advances in sensing plant diseases for precision crop protection. *European Journal of Plant Pathology* **133**, 197-209 (2012).
49. D. Tholl, O. Hossain, A. Weinhold, U. S. R. Röse, Q. Wei, Trends and applications in plant volatile sampling and analysis. *The Plant Journal* **106**, 314-325 (2021).
50. S. Cui, P. Ling, H. Zhu, H. M. Keener, Plant pest detection using an artificial nose system: a review. *Sensors* **18**, 378 (2018).
51. M. Ray *et al.*, Fungal disease detection in plants: Traditional assays, novel diagnostic techniques and biosensors. *Biosens Bioelectron* **87**, 708-723 (2017).
52. R. Ghaffari *et al.*, Plant pest and disease diagnosis using electronic nose and support vector machine approach. *Journal of Plant Diseases and Protection* **119**, 200-207 (2012).
53. B. Zhou, J. Wang, Discrimination of different types damage of rice plants by electronic nose. *Biosystems Engineering* **109**, 250-257 (2011).

54. F. Spinelli, M. Noferini, J. L. Vanneste, G. Costa, Potential of the electronic-nose for the diagnosis of bacterial and fungal diseases in fruit trees. *EPPO Bulletin* **40**, 59-67 (2010).
55. J. Laothawornkitkul *et al.*, Discrimination of Plant Volatile Signatures by an Electronic Nose: A Potential Technology for Plant Pest and Disease Monitoring. *Environmental Science & Technology* **42**, 8433-8439 (2008).
56. Z. Li *et al.*, Real-time monitoring of plant stresses via chemiresistive profiling of leaf volatiles by a wearable sensor. *Matter* **4**, 2553-2570 (2021).
57. M. J. Anderson, J. G. Sullivan, T. K. Horiuchi, S. B. Fuller, T. L. Daniel, A bio-hybrid odor-guided autonomous palm-sized air vehicle. *Bioinspiration & Biomimetics* **16**, 026002 (2020).
58. S. Neta, G. Ariel, Y. Yossi, A. Amir, M. M. Ben, The Locust antenna as an odor discriminator. *Biosensors and Bioelectronics* **221**, 114919 (2023).
59. C. Geckeler, S. E. Ramos, M. C. Schuman, S. Mintchev, Robotic volatile sampling for early detection of plant stress: Precision agriculture beyond visual remote sensing. *IEEE Robotics & Automation Magazine*, 2-12 (2023).
60. K. Minami, K. Shiba, G. Yoshikawa, Sorption-induced static mode nanomechanical sensing with viscoelastic receptor layers for multistep injection-purge cycles. *Journal of Applied Physics* **129**, (2021).
61. J. Krechmer *et al.*, Evaluation of a new reagent-ion source and focusing ion–molecule reactor for use in proton-transfer-reaction mass spectrometry. *Analytical Chemistry* **90**, 12011-12018 (2018).
62. The American Society of Mechanical Engineers (ASME), Weed-fighting robots could replace spraying (2018); https://www.asme.org/topics-resources/content/weedfighting-robots-could-replace-spraying
63. W. A. Gardner, J. R. Fuxa, Pathogens for the suppression of the fall armyworm. *The Florida Entomologist* **63**, 439-447 (1980).
64. P. Fallet *et al.*, Laboratory and field trials reveal the potential of a gel formulation of entomopathogenic nematodes for the biological control of fall armyworm caterpillars (*Spodoptera frugiperda*). *Biological Control* **176**, 105086 (2022).
65. C. M. Arce, G. Besomi, G. Glauser, T. C. J. Turlings, Caterpillar-induced volatile emissions in cotton: the relative importance of damage and insect-derived factors. *Frontiers in Plant Science* **12**, (2021).
66. D. Balmer, D. V. de Papajewski, C. Planchamp, G. Glauser, B. Mauch-Mani, Induced resistance in maize is based on organ-specific defence responses. *Plant J* **74**, 213-225 (2013).
67. T. C. J. Turlings, P. J. McCall, H. T. Alborn, J. H. Tumlinson, An elicitor in caterpillar oral secretions that induces corn seedlings to emit chemical signals attractive to parasitic wasps. *J Chem Ecol* **19**, 411-425 (1993).
68. T. C. J. Turlings, A. C. Davison, C. Tamò, A six-arm olfactometer permitting simultaneous observation of insect attraction and odour trapping. *Physiol. Entomol.* **29**, 45-55 (2004).
69. MSS Alliance, Press Release (2015.09.29): MSS Alliance Launched to Set De Facto Standard for Odor-Sensing Systems (2015); https://www.nims.go.jp/eng/news/press/2015/10/201510130.html
70. MSS Forum, Press Release (2017.10.16): ”MSS Forum" launched to promote the establishment of a de facto standard for olfactory iot sensing systems (2017); https://www.nims.go.jp/eng/news/press/2017/10/201710160.html
71. H. Li *et al.*, Terpenes and their oxidation products in the French Landes forest: insights from

Vocus PTR-TOF measurements. *Atmos. Chem. Phys.* **20**, 1941-1959 (2020).

72. T. C. J. Turlings, J. H. Tumlinson, Systemic release of chemical signals by herbivore-injured corn. *Proceedings of the National Academy of Sciences of the United States of America* **89**, 8399-8402 (1992).
73. F. J. Oksanen *et al.*, Vegan: Community Ecology Package, 2.6-4 (2022); https://cran.r-project.org/web/packages/vegan/index.html
74. A. Liaw, M. Wiener, Classification and regression by random forest. *R News* **2**, 18-22 (2002).
75. E. Archer, rfPermute: Estimate permutation p-values for random forest importance metrics. R package 2.5.2 (2023); https://cran.r-project.org/web/packages/rfPermute/index.html
76. T. Chen *et al.*, xgboost: Extreme Gradient Boosting. R package version, 1.7.5.1 (2023); https://CRAN.R-project.org/package=xgboost
77. M. Kuhn, Building predictive models in R using the caret Package. *Journal of Statistical Software* **28**, 1-26 (2008).
78. K. Buhr, S. van Ruth, C. Delahunty, Analysis of volatile flavour compounds by Proton Transfer Reaction-Mass Spectrometry: fragmentation patterns and discrimination between isobaric and isomeric compounds. *International Journal of Mass Spectrometry* **221**, 1-7 (2002).
79. X. Pang, Biogenic volatile organic compound analyses by PTR-TOF-MS: Calibration, humidity effect and reduced electric field dependency. *Journal of Environmental Sciences* **32**, 196-206 (2015).
80. D. Pagonis, K. Sekimoto, J. de Gouw, A library of proton-transfer reactions of H3O+ ions used for trace gas detection. *Journal of The American Society for Mass Spectrometry* **30**, 1330-1335 (2019).
81. E. Kari, P. Miettinen, P. Yli-Pirilä, A. Virtanen, C. L. Faiola, PTR-ToF-MS product ion distributions and humidity-dependence of biogenic volatile organic compounds. *International Journal of Mass Spectrometry* **430**, 87-97 (2018).
82. A. M. Yáñez-Serrano *et al.*, GLOVOCS - Master compound assignment guide for proton transfer reaction mass spectrometry users. *Atmospheric Environment* **244**, 117929 (2021).

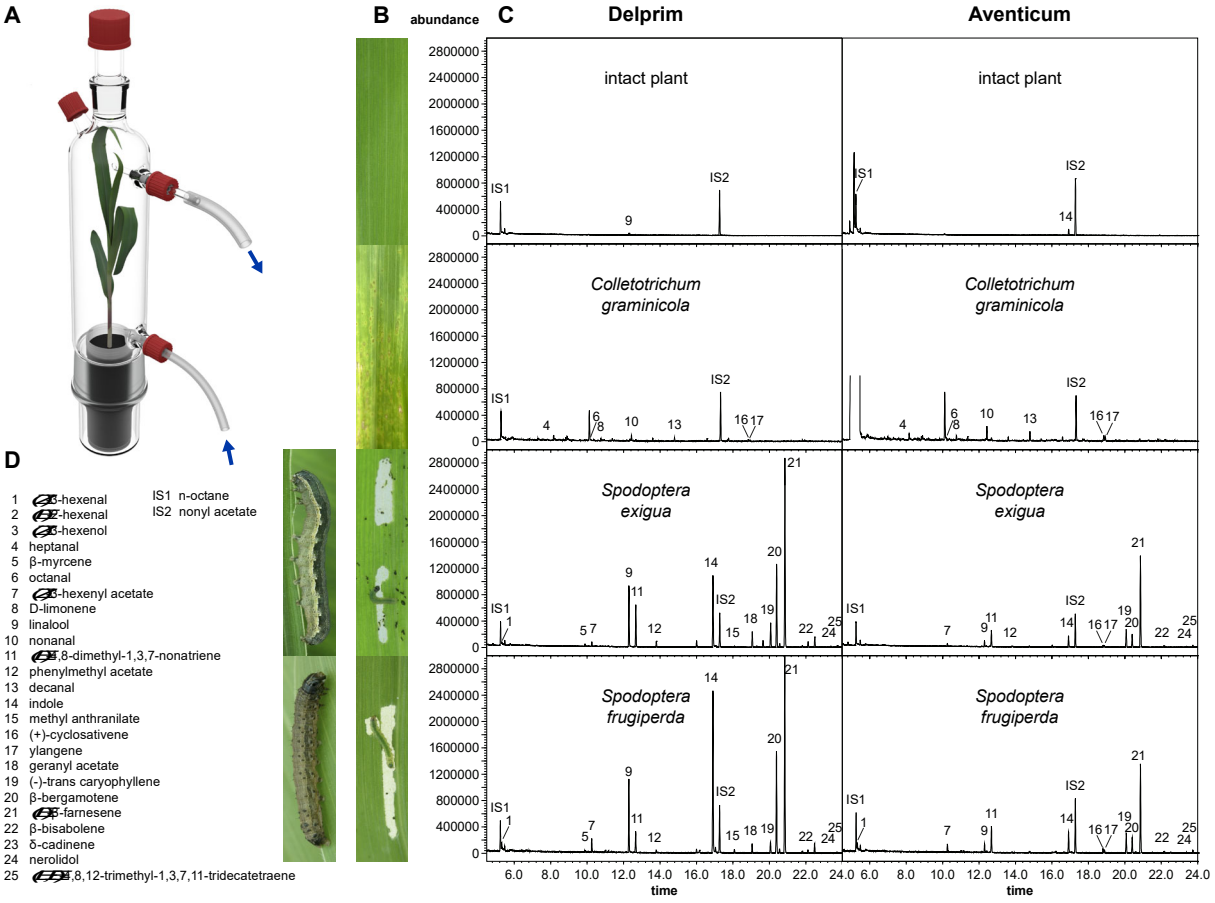

Fig. 1. Volatile profiles of caterpillar- and pathogen-infested maize plants. (**A**) Experimental set-up that was used to collect volatiles from plants enclosed in glass vessels. (**B**) Pictures of the different treatments: an undamaged leaf and leaves with damage inflicted by two herbivores and a pathogen. (**C**) examples of chromatograms obtained by GC-MS analyses (total ion counts). (**D**) List of the main volatile compounds.

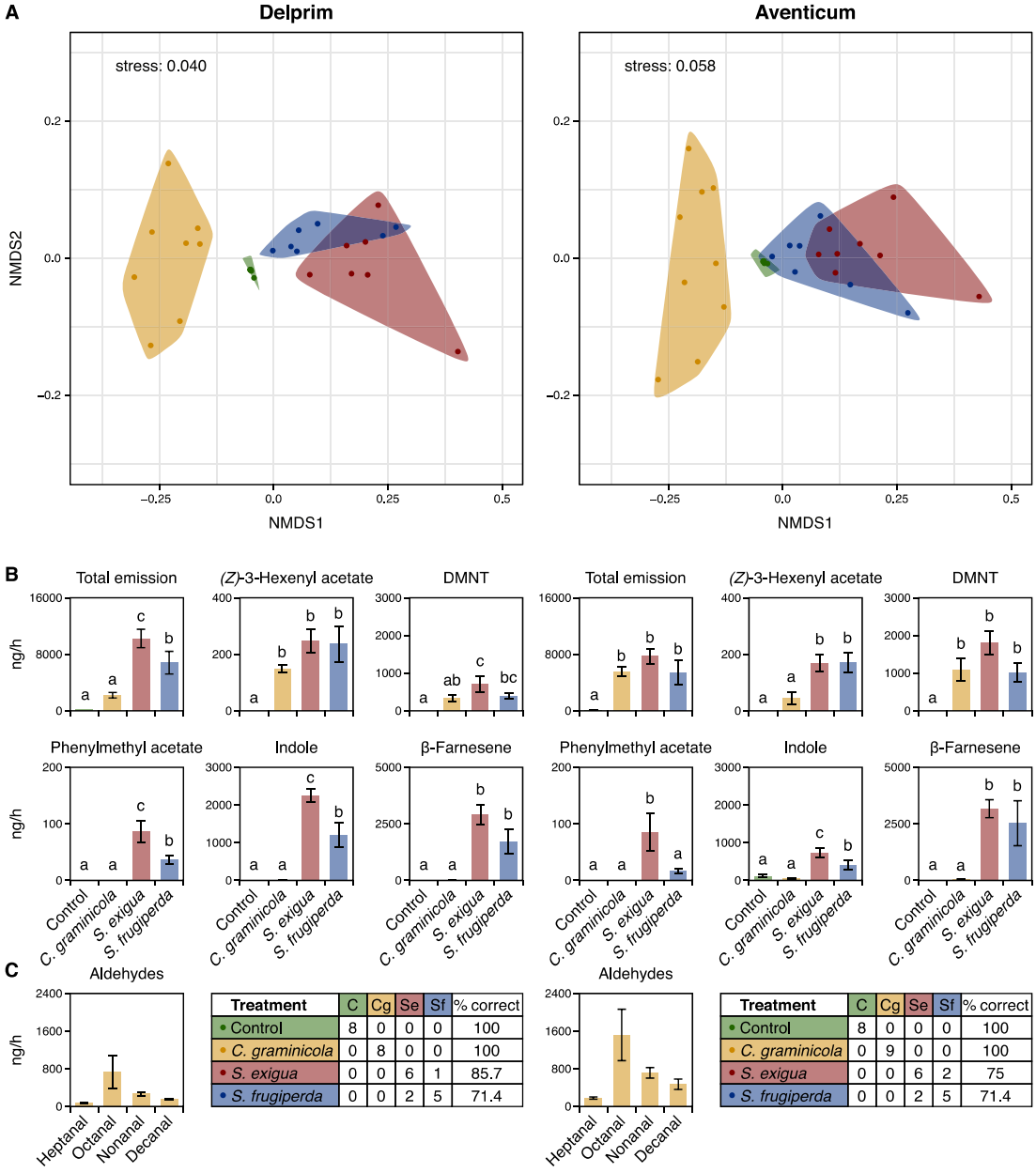

Fig. 2. Characterization of the volatile profiles of maize plants infested with different pests using classical gas chromatography-mass spectrometry (GC-MS) under laboratory conditions. Undamaged (in green) maize plants of the varieties Delprim and Aventicum were compared to plants infested with a fungal pathogen (*Colletotrichum graminicola*; in yellow) and caterpillars (*Spodoptera exigua* in red and *Spodoptera frugiperda* in blue). (**A**) Nonmetric multidimensional scaling analysis (NMDS) plot. (**B**) Quantities in ng/h (mean ± s.e.) of the main

669 volatiles differing between treatments. Different letters indicate significant pairwise comparisons
670 after multiple test adjustment (FDR). (**C**) Confusion matrix summarizing the performance of a
671 Random Forest classification, indicating the correctness in assigning measurements to a
672 particular treatment.

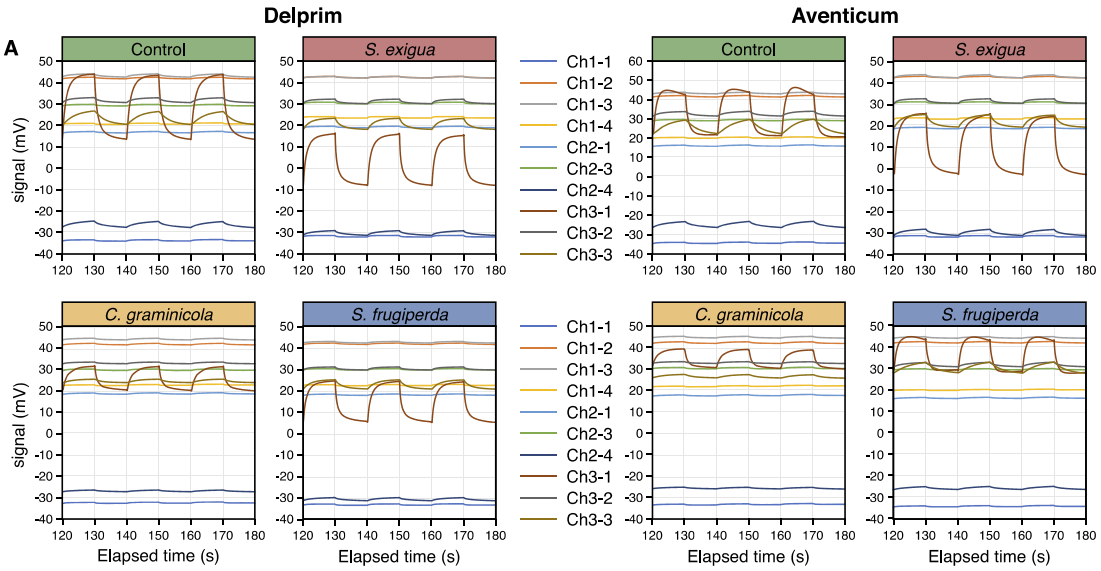

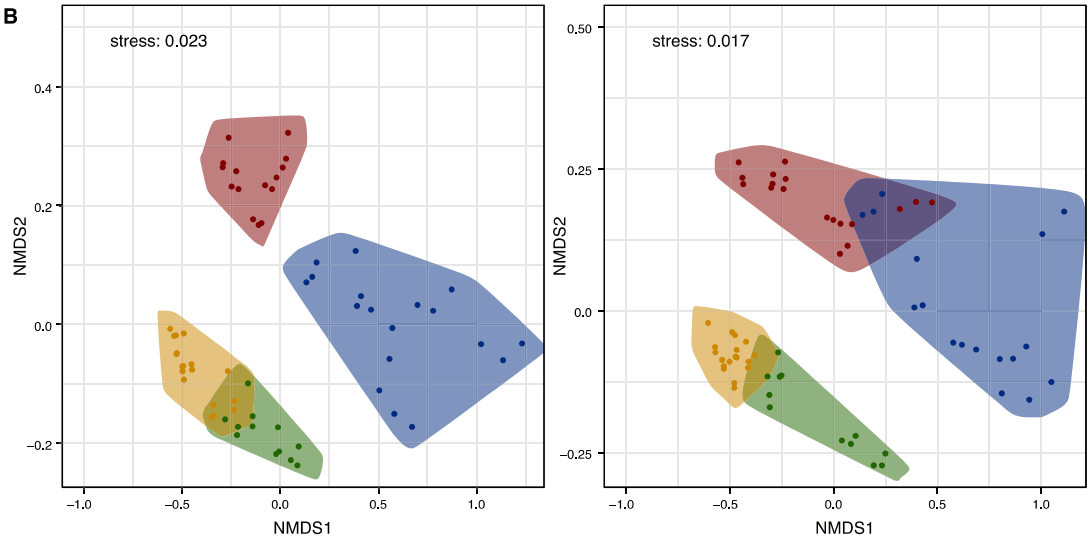

C

Treatment	C	Cg	Se	Sf	% correct
Control	11	1	0	0	91.7
C. graminicola	0	18	0	0	100
S. exigua	0	0	15	0	100
S. frugiperda	0	0	0	18	100

Treatment	C	Cg	Se	Sf	% correct
Control	12	0	0	0	100
C. graminicola	0	18	0	0	100
S. exigua	0	0	17	1	94.4
S. frugiperda	0	0	1	16	94.1

Fig. 3. Discrimination among the volatile profiles of maize plants infested with different pests using a membrane-type surface stress (MSS) sensor under laboratory conditions. Undamaged (in green) maize plants of the varieties Delprim and Aventicum were compared to plants infested with a fungal pathogen (*Colletotrichum graminicola*; in yellow) and caterpillars (*Spodoptera exigua* in red and *Spodoptera frugiperda* in blue). (**A**) Signals recorded during three cycles of sampling-purging from ten independent disks coated with different adsorbent polymers. (**B**) Nonmetric multidimensional scaling analysis (NMDS) plot. (**C**) Confusion matrix

681 summarizing the performance of a Random Forest classification, indicating the correctness in
682 assigning measurements to a particular treatment.
683

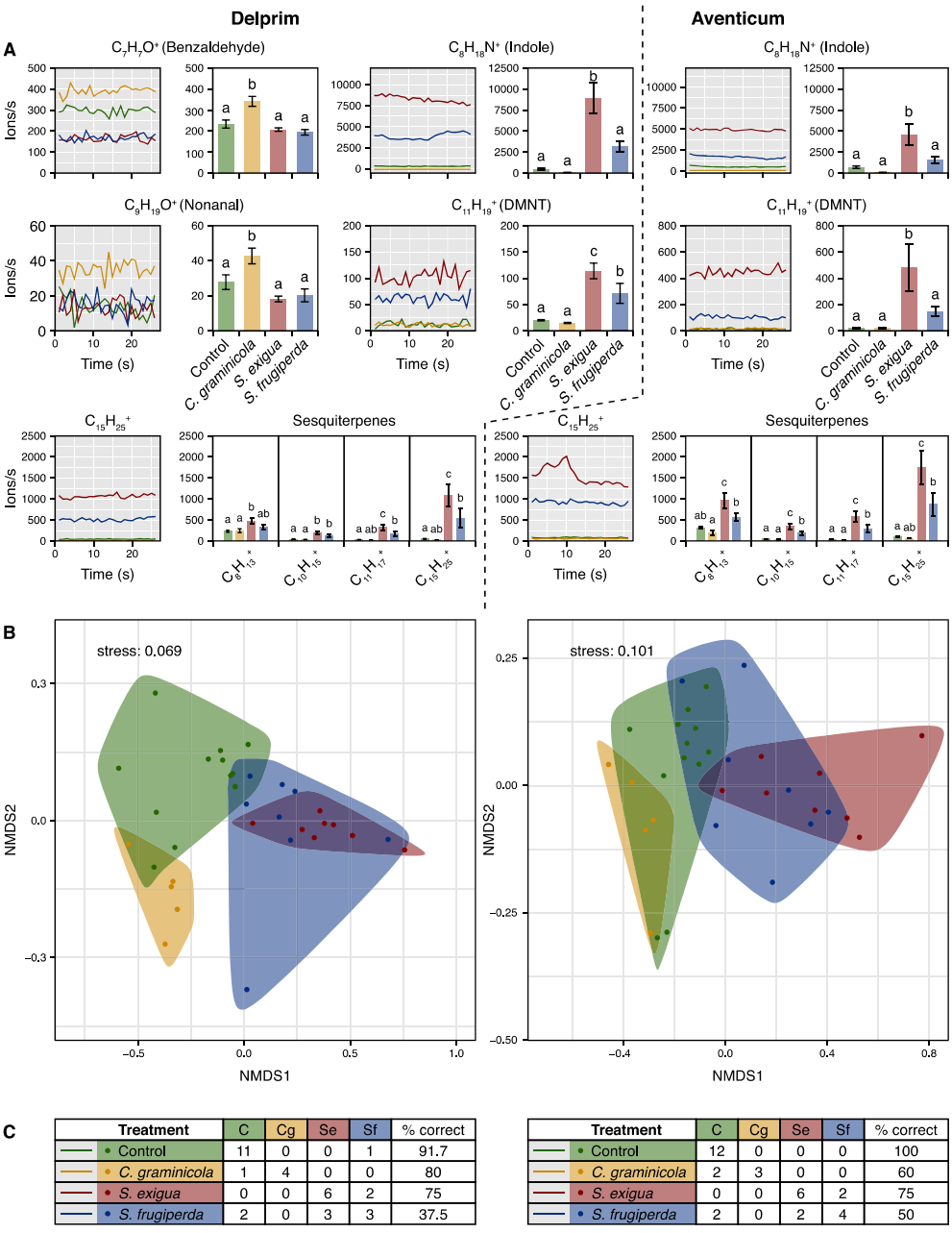

Treatment	C	Cg	Se	Sf	% correct
Control	11	0	0	1	91.7
C. graminicola	1	4	0	0	80
S. exigua	0	0	6	2	75
S. frugiperda	2	0	3	3	37.5

Treatment	C	Cg	Se	Sf	% correct
Control	12	0	0	0	100
C. graminicola	2	3	0	0	60
S. exigua	0	0	6	2	75
S. frugiperda	2	0	2	4	50

Fig. 4. Discrimination among the volatile profiles of maize plants infested with different pests using a proton-transfer-reaction time-of-flight mass spectrometer (PTR-TOF-MS) under laboratory conditions. Undamaged (in green) maize plants of the varieties Delprim and Aventicum were compared to plants infested with a fungal pathogen (*Colletotrichum graminicola*; in yellow) and caterpillars (*Spodoptera exigua* in red and *Spodoptera frugiperda* in blue). (**A**) Raw signals (ion counts per seconds) and the quantile 0.9 (mean ± s.e.) measured over

25 seconds for some of the volatiles (protonated parent and fragment masses) that showed differences between treatments. Different letters indicate significant pairwise comparisons after multiple test adjustment (FDR). (**B**) Nonmetric multidimensional scaling analysis (NMDS) plot. (**C**) Confusion matrix summarizing the performance of a Random Forest classification, indicating the correctness in assigning measurements to a particular treatment.

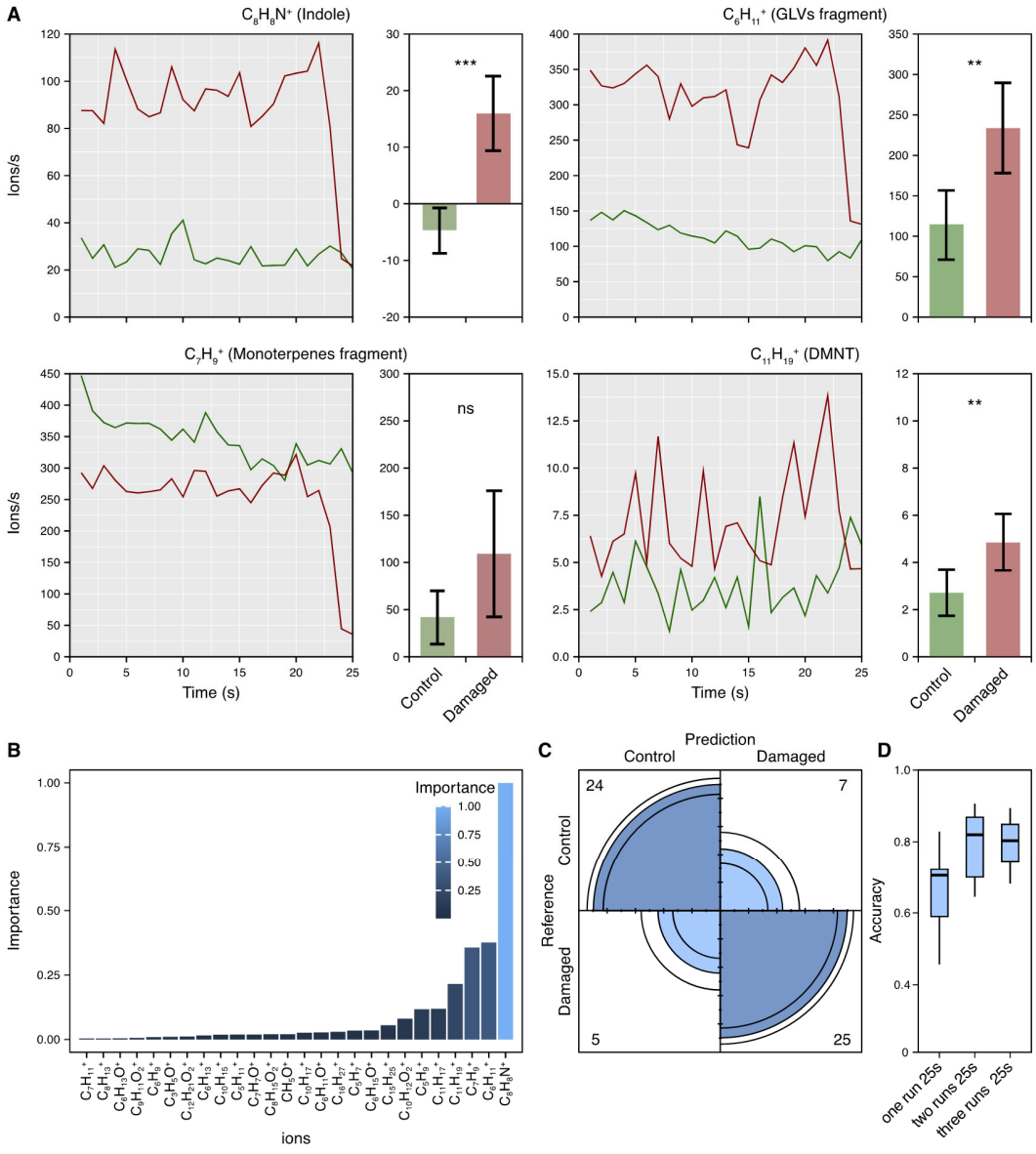

Fig. 5. Discrimination between volatile emissions from undamaged and damaged plants under outdoor conditions using a proton-transfer-reaction time-of-flight mass spectrometer (PTR-TOF-MS) and Extreme Gradient Boosting modelling. Undamaged (in green) maize plants of the variety Delprim were compared to plants with simulated caterpillar damage (in red). (**A**) Raw signals (ion counts per seconds) and the quantile 0.9 (after subtraction of background odors, mean ± s.e.) of the volatiles (protonated parent or fragment masses) ranked as the four most important predictors in the model. Statistically significant differences (Wilcoxon test) are denoted by ** = $p < 0.01$ and *** = $p < 0.001$. (**B**) Importance of variables (ions) in the Extreme Gradient Boosting model to discriminate intact and damaged plants. (**C**) Confusion matrix

summarizing the performance of the model using three runs of measurement for each plant. (**D**) Sensitivity analysis assessing the model's performance with different measurement runs for each treatment (median ± s.d.).